Copy 247



NASA TM X-816

19p.

X63 13225

Code

(NASA-TM-X-816) AN EXPLORATORY INVESTIGATION AT A MACH NUMBER OF 6.9 INTO THE USE OF AERODYNAMIC CONTROLS FOR MODULATING THE LIFT-DRAG RATIO OF AN APOLLO TYPE L. Neal, Jr. (NASA) May 1963 19 p 00/99 N72-73351 Unclas 32192

# TECHNICAL MEMORANDUM

X-816

## AN EXPLORATORY INVESTIGATION AT A MACH NUMBER OF 6.9 INTO THE USE OF AERODYNAMIC CONTROLS FOR MODULATING THE LIFT-DRAG RATIO OF AN APOLLO TYPE CONFIGURATION

By Luther Neal, Jr.

Langley Research Center
Langley Station, Hampton, Va.

CLASSIFICATION CHANGED
UNCLASSIFIED
By Authority of ID-72-234 Date 6/18/72

NATIONAL AERONAUTICS AND SPACE ADMINISTRATION

WASHINGTON

May 1963

NATIONAL AERONAUTICS AND SPACE ADMINISTRATION

TECHNICAL MEMORANDUM X-816

# AN EXPLORATORY INVESTIGATION AT A MACH NUMBER OF 6.9 INTO THE USE OF AERODYNAMIC CONTROLS FOR MODULATING THE LIFT-DRAG RATIO OF AN APOLLO TYPE CONFIGURATION*

By Luther Neal, Jr.

## SUMMARY

An investigation has been conducted in the Langley 11-inch hypersonic tunnel at a Mach number of 6.9 and a Reynolds number of about 440,000 to determine the suitability of various aerodynamic controls on an Apollo type capsule over an angle-of-attack range from -5° to 33°. The controls investigated consisted of several chin and afterbody flaps and a series of hinged cylinders attached to the model base. The moment reference of the basic model was located off the axis of symmetry to permit the vehicle to trim at a nominal lift-drag ratio of approximately -0.5 and then the effectiveness of the various controls in providing trim at reduced ratios was determined. The results of the study indicate that base-mounted cylindrical controls are relatively ineffective in terms of control area required. The effectiveness of the flap controls is strongly dependent on their location.

## INTRODUCTION

The lift-drag ratio of a manned vehicle returning from a lunar mission must be modulated during reentry in order to alleviate the heat-protection problem and to obtain the desired range maneuverability. In the present Apollo concept, lift capability is to be provided by offsetting the center of gravity from the axis of symmetry a sufficient amount to allow the vehicle to trim at a nominal lift coefficient. The lift-drag ratio will then be modulated by use of the fixed-pitch—variable-roll technique as discussed in reference 1. The current study was undertaken to explore aerodynamic control systems capable of providing a similar lift-modulation capability.

Several schemes for obtaining lift on blunt-body low lift-drag ratio configurations have previously been investigated. (See refs. 2 to 6.) The effectiveness of control devices such as chin flaps, afterbody flaps, and nose spikes was

determined at Mach 9.6 from the investigation reported in reference 2 for blunt-body configurations of various forebody geometry and the Mercury afterbody. Other studies of the effectiveness of various aerodynamic controls on Mercury type capsules are reported in references 3 and 4. A summary of aerodynamic characteristics for several reentry vehicles capable of obtaining hypersonic lift-drag ratios on the order of 0.5 from subsonic to hypersonic speeds is given in reference 6. Various types of controls were utilized throughout the investigation to determine trim and control characteristics of the vehicles.

Because of configuration differences, little of this information is directly applicable to the Apollo vehicle. The present investigation was initiated to supply hypersonic wind-tunnel data on the suitability of various kinds and locations of aerodynamic controls on an Apollo-type vehicle.

## SYMBOLS

$C_{A,b}$ balance chamber axial-force coefficient, $\frac{(p - p_b)}{qS} S_b$

$C_D$ drag coefficient, $\frac{\text{Drag}}{qS}$

$C_L$ lift coefficient, $\frac{\text{Lift}}{qS}$

$C_m$ pitching-moment coefficient, $\frac{\text{Pitching moment}}{qSd}$

$\Delta C_m$ increment pitching-moment coefficient over basic body value

$\frac{L}{D}$ lift-drag ratio

$d$ maximum diameter of basic model (fig. 2), in.

$l$ length of cylindrical flaps (fig. 2), in.

$M$ free-stream Mach number

$p$ free-stream static pressure, lb/sq in.

$p_b$ average pressure acting inside balance shield, lb/sq in.

$S$ maximum cross-sectional area of model, $\frac{\pi}{4} d^2$, sq in.

$S_b$ outside area of balance shield, sq in.

$S_c$ exposed planform area of control surfaces, sq in.

$q$ free-stream dynamic pressure, lb/sq in.

$x$ surface distance measured from nose center line (fig. 10), in.

$\alpha$ angle of attack (fig. 2), deg

$\delta_c$ control deflection angle (fig. 2), deg

## APPARATUS AND TESTS

A photograph of the basic reentry configuration studied is shown in figure 1. Detail drawings of the model and the various control surfaces investigated are given in figure 2. The only difference between flap 3 and flap 4 was the amount of exposed area since flap 4 was embedded further into the model than flap 3 in order to form a more realistic hinge-line location. In selecting the cylindrical flaps, consideration was given to the fact that the internal volume of these flaps might possibly be utilized for storage space. A narrow slot was cut in the rear of the model to permit the cylindrical flaps to be pivoted about the center of the spherical body base. The unoccupied portion of all slots and holes was filled with dental plaster and refinished prior to each run to obtain the original model geometry as indicated in the figure.

The tests were conducted in the $M = 6.8$ Invar nozzle of the Langley 11-inch hypersonic tunnel. A description of the tunnel is given in reference 7 and a calibration of the nozzle may be found in reference 8. The test-section Mach number varies slightly with tunnel stagnation pressure because of changes in tunnel-wall boundary-layer thickness.

The present tests were conducted at an average stagnation pressure of 18.7 atmospheres which resulted in an average Mach number of 6.9. The stagnation temperature was maintained at about 650° F which was sufficient to prevent the liquefaction of air in the test section. The resulting Reynolds number based on body diameter and corresponding to these test conditions was about 440,000.

The forces and moments on the model were measured with a six-component strain-gage balance. The balance was inserted into the model at 33° to the center line in order to permit mounting of cylindrical flaps at the base of the model. The true angle of attack was obtained irrespective of any load deflection by optical means in which a small prism mounted on the model reflected a point source of light on a calibrated scale. The pressure acting inside the balance shield was measured during each test run; however, no correction for these pressures was applied to the data since calculations showed that such corrections were small ($-0.003 < C_{A,b} < 0$). The variation in dynamic pressure due to slight changes in Mach number with time for the nozzle used is about ±2 percent and was accounted for in the reduction of the data.

## DISCUSSION OF RESULTS

The longitudinal aerodynamic characteristics referred to stability axes are shown in figures 3 to 8 for the configuration with various types of controls. With the moment reference located at the position indicated in figure 2, the basic body trimmed at an angle of attack of approximately 31.5° which corresponds to a trim L/D of -0.48. Reduction of this negative trim L/D resulting from the use of aerodynamic controls will be referred to as "flap effectiveness" throughout the report. The greater part of the lift modulation results from changes in trim angle of attack rather than from direct load on the control surfaces.

General examination of the basic data for the configuration with the various controls indicates, as in the tests of reference 2, that a control located near the rim of the capsule is much more effective, in terms of control area required, than those located rearward along the afterbody. The effects of flap area on L/D modulation capability are best illustrated for the various control surfaces in the summary plot in figure 9. For the cases shown here, trimmed L/D is generally much more affected by variation in the chin flap area (fig. 9(a)) than by variation in the area of the afterbody (fig. 9(b)) or cylindrical flaps (fig. 9(c)). However a considerable reduction in chin flap effectiveness occurs at location 2 over that at location 1. From the spread in L/D trim between the various flap deflections, it is apparent that maximum effectiveness of the chin flaps occurs at flap deflections greater than 90°. It is shown in the data of references 2 and 9 that maximum effectiveness for chin flaps on Mercury type bodies occurred near flap deflections of 140°. Maximum effectiveness has been reached within the 90° flap-deflection range for the smaller afterbody flaps but not for the large one. For the cylindrical flaps, the increment in L/D modulation capability obtained by increasing the flap deflection from 29° to 55° is small for the small cylinders but generally tends to increase with increasing control area.

It must be pointed out that the taper ratios of the chin and afterbody flaps and the fineness ratios of the cylindrical flaps vary with area changes; therefore, the entire effects shown in figure 9 are not derived from area changes alone. Nevertheless, the general trends shown should represent qualitative effects from changes in flap area.

In order to show the general trend of the effect of location on flap effectiveness the data in figures 9(a) and 9(b) were faired and a cross plot was made at $S_c/S = 0.097$ which is shown in figure 10(a). For flap deflections of 45° and 57°, a flap of this size just behind the lip of the model is no more effective than an afterbody flap; however, for a flap deflection of 90°, the effectiveness decreases with increases in x/d for the three cases shown here. Untrimmed increments in pitching-moment coefficient obtained from cross plots for the same flap area ratio are shown in figure 10(b) for several angles of attack. In general, the decline in pitching-moment increment with increasing x/d is, at all angles of attack, similar to the loss in effectiveness in modulating trim L/D. (See fig. 10(a).)

Typical schlieren photographs are shown in figure 11. For angles of attack near 30°, the bow shock intersected the longer cylindrical flaps for large control

deflections as shown for flap 13, $\delta_c = 55^\circ$, $\alpha = 30^\circ$. Similar bow shock impingement also occurred for large flap deflections of the afterbody flaps as seen for flap 6, $\delta_c = 90^\circ$, $\alpha = 30^\circ$.

## CONCLUDING REMARKS

The concluding remarks that follow result from the analysis of a force and moment investigation at a Mach number of 6.9, a Reynolds number of 440,000, and an angle-of-attack range from $-5^\circ$ to $33^\circ$ on an Apollo type reentry vehicle.

Chin flaps with a cross-sectional area equal to about 9 percent of the model frontal area provided lift modulation over a lift-drag-ratio range from -0.48 to 0 when deflected $90^\circ$; greater effectiveness could be obtained by increasing the flap deflection. A similar flap located on the afterbody was approximately half as effective as the rim-located chin flap. A slight rearward movement in the chin flap resulted in a considerable loss in effectiveness. It was possible to trim the vehicle at L/D values near zero through the use of base-mounted cylinders, but the required area in the axial plane of the cylinder was approximately one-third the frontal area of the model.

Langley Research Center,
National Aeronautics and Space Administration,
Langley Station, Hampton, Va., March 4, 1963.

## REFERENCES


1. Becker, J. V., Baradell, D. L., and Pritchard, E. B.: Aerodynamics of Trajectory Control for Re-Entry at Escape Speed. Astronautica Acta, Vol. VII, Fasc. 5-6, 1961, pp. 334-358.

2. Armstrong, William O.: Effect of Various Forebody Modifications on the Static Longitudinal Stability and Control Characteristics of a Reentry Capsule at a Mach Number of 9.6. NASA TM X-469, 1961.

3. Sammonds, Robert I., and Dickey, Robert R.: Effectiveness of Several Control Arrangements on a Mercury-Type Capsule. NASA TM X-579, 1961.

4. Tendeland, Thorval, and Pearson, B. Douglas, Jr.: Effectiveness of Two Flap Controls on a Mercury Type Capsule at a Mach Number of 15 in the Ames Hypersonic Helium Tunnel. NASA TM X-660, 1962.

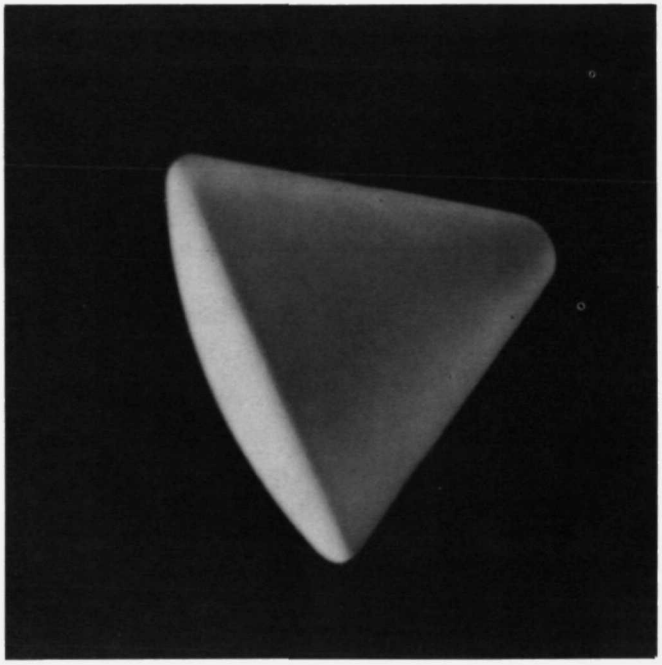
5. Intrieri, Peter F.: Effects of Transverse Center-of-Gravity Displacement, Afterbody Geometry, and Front-Face Curvature on the Aerodynamic Characteristics of Mercury-Type Models at a Mach Number of 5.5. NASA TM X-569, 1961.

6. Rainey, Robert W., Complier: Summary of Aerodynamic Characteristics of Low-Lift-Drag-Ratio Reentry Vehicles From Subsonic to Hypersonic Speeds. NASA TM X-588, 1961.

7. McLellan, Charles H., Williams, Thomas W., and Bertram, Mitchel H.: Investigation of a Two-Step Nozzle in the Langley 11-Inch Hypersonic Tunnel. NACA TN 2171, 1950.

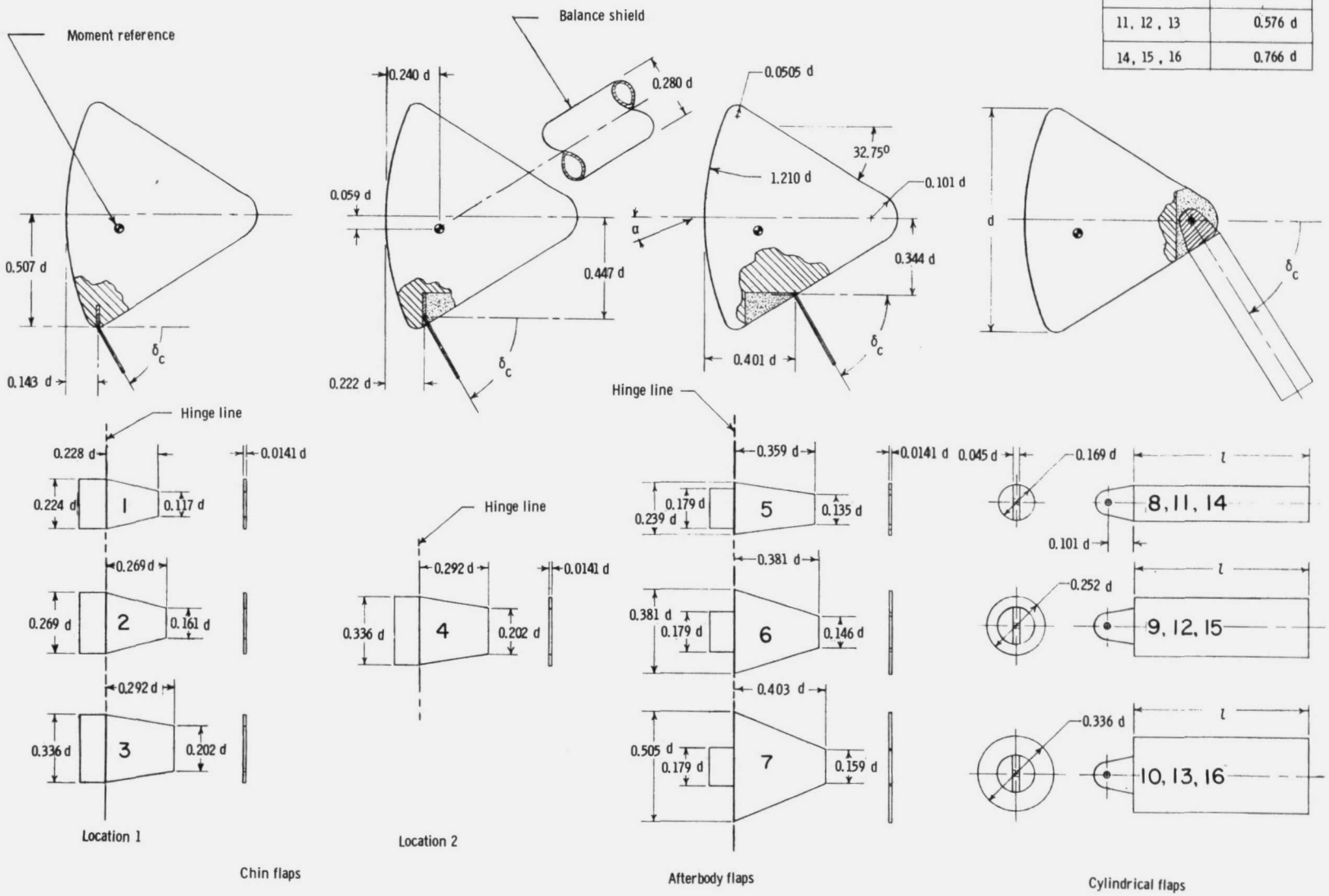
8. Bertram, Mitchel H.: Exploratory Investigation of Boundary-Layer Transition on a Hollow Cylinder at a Mach Number of 6.9. NACA Rep. 1313, 1957. (Supersedes NACA TN 3546.)

9. Penland, Jim A., and Armstrong, William O.: Static Longitudinal Aerodynamic Characteristics of Several Wing and Blunt-Body Shapes Applicable for Use as Reentry Configurations at a Mach Number of 6.8 and Angles of Attack up to $90^{\circ}$. NASA TM X-65, 1959.



L-63-77

Figure 1.- Photograph of the basic body.




| Control | l |
|---|---|
| 8, 9, 10 | 0.384 d |
| 11, 12, 13 | 0.576 d |
| 14, 15, 16 | 0.766 d |

Figure 2.- Detail drawing of the model and control devices. d = 2.230 inches.

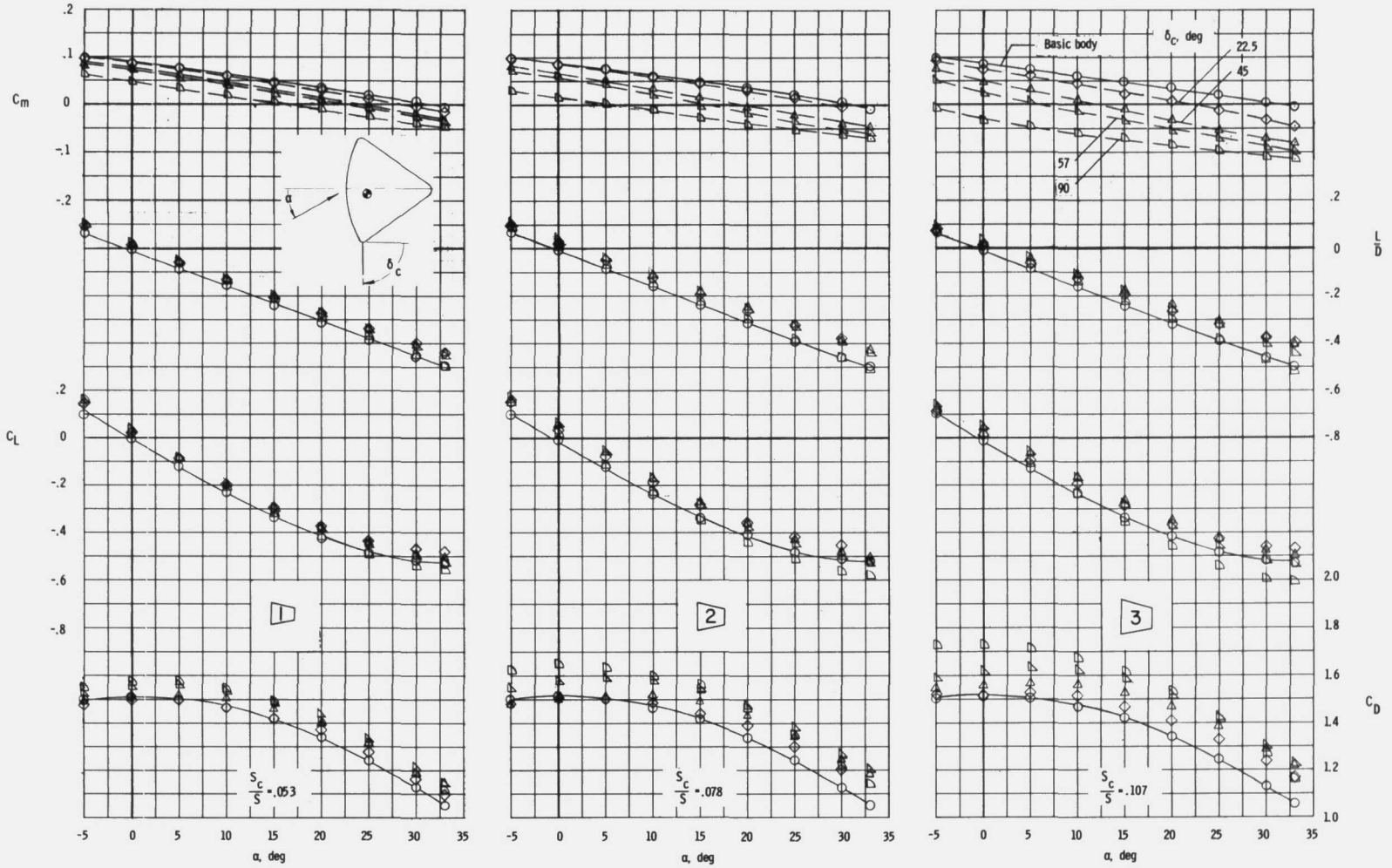



Figure 3.- Longitudinal aerodynamic characteristics of the configuration with chin flaps at location 1.

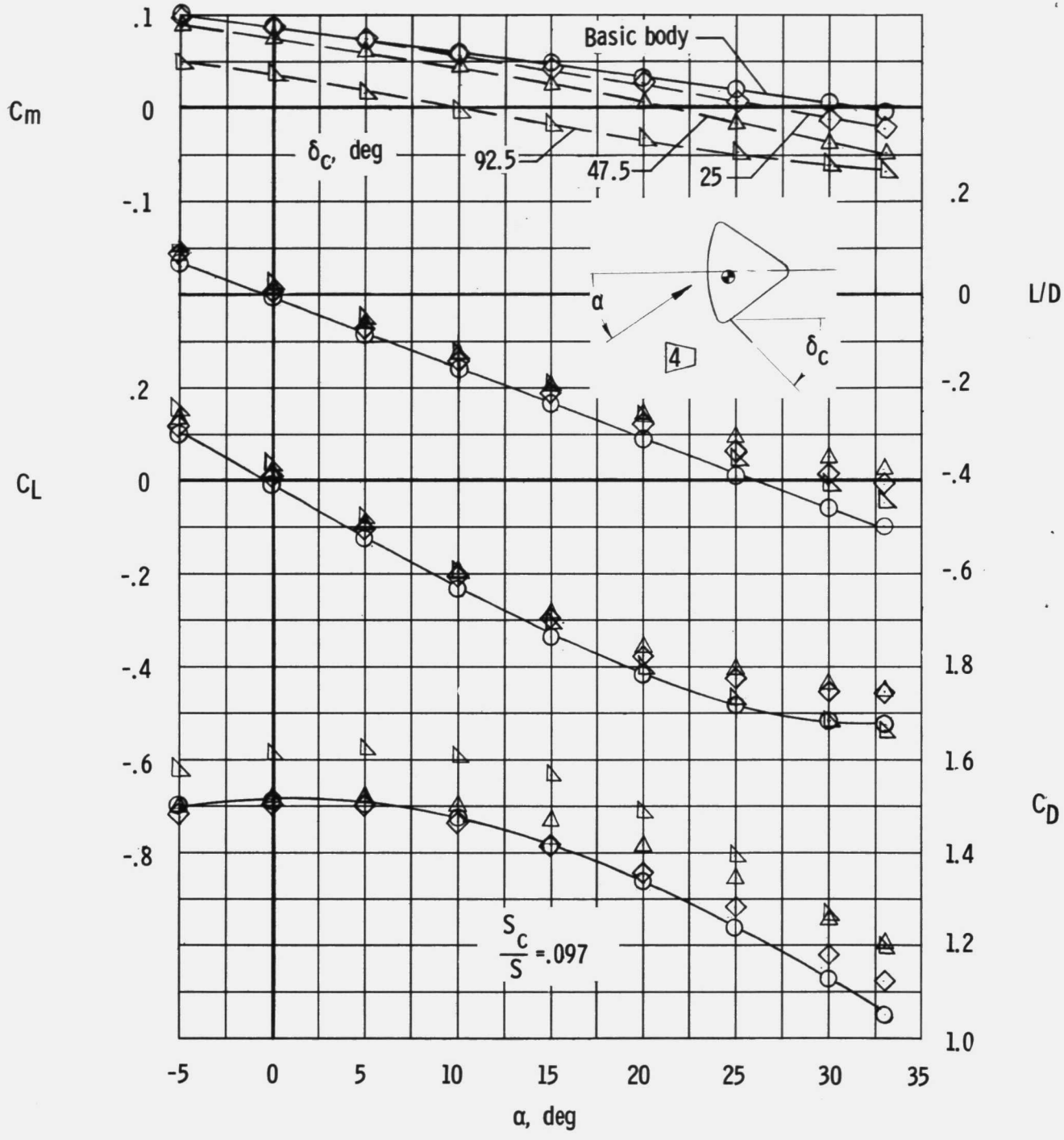



Figure 4.- Longitudinal aerodynamic characteristics of the configuration with chin flap 4 at location 2.

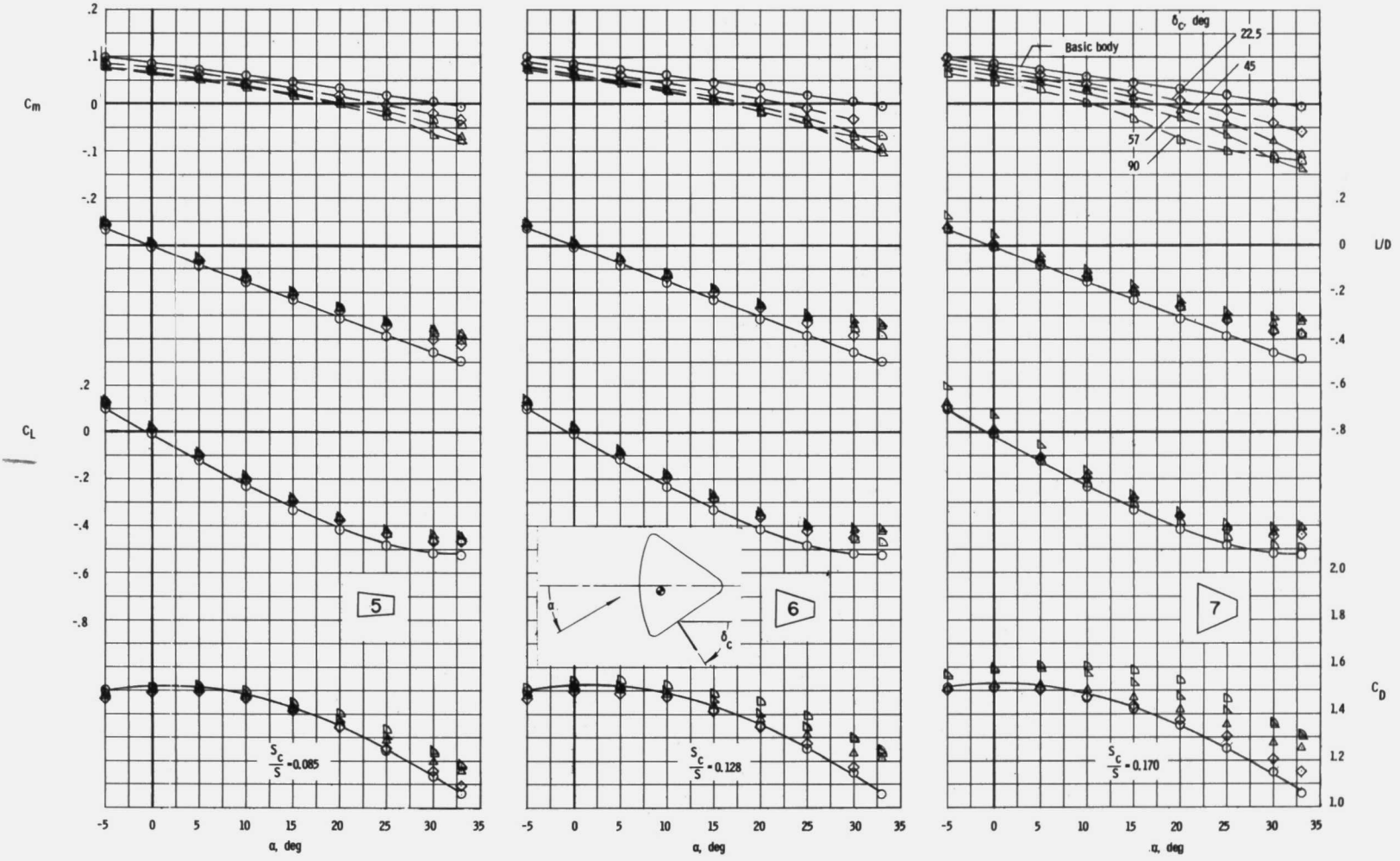



Figure 5.- Longitudinal aerodynamic characteristics of the configuration with afterbody flaps.

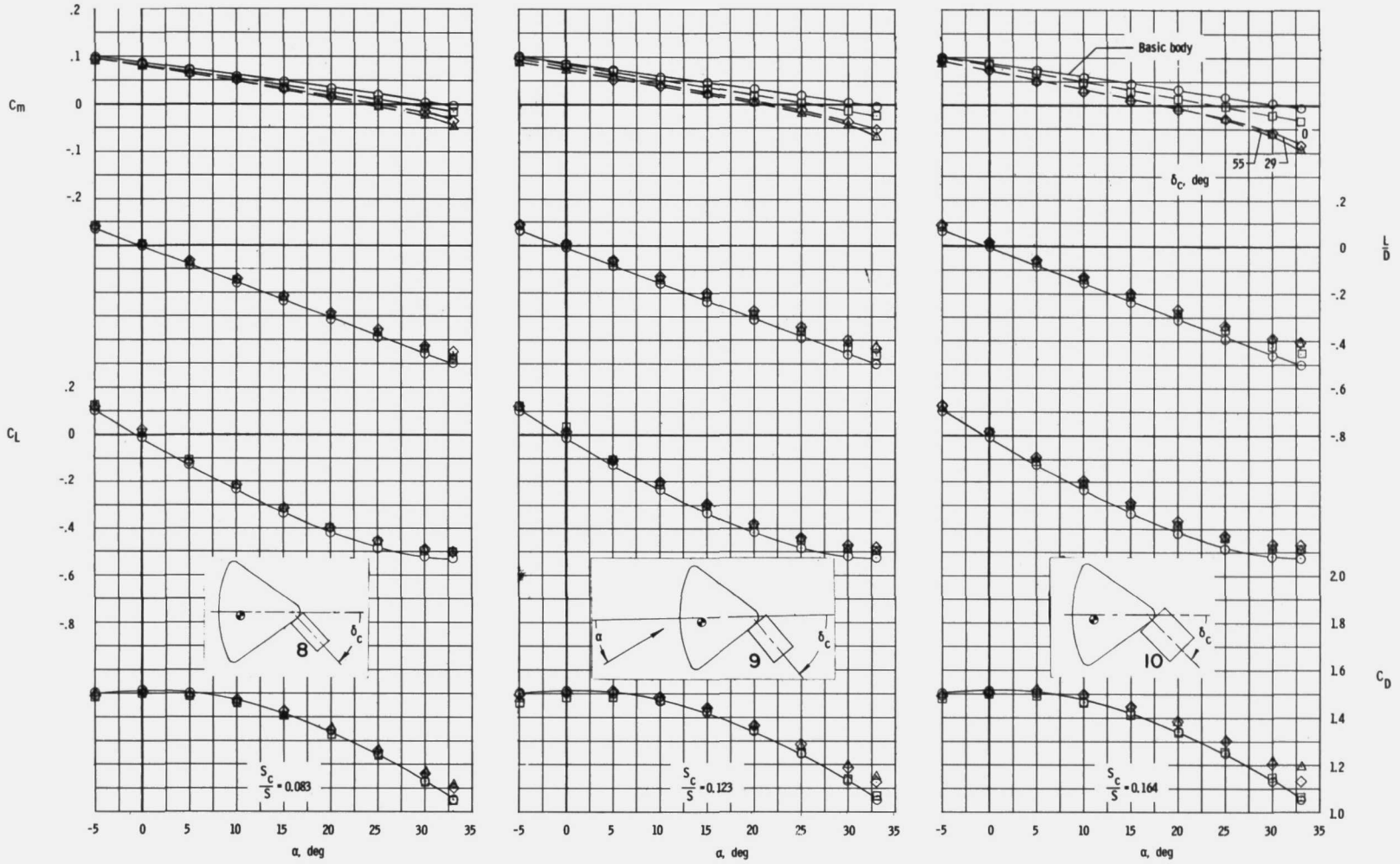



Figure 6.- Longitudinal aerodynamic characteristics of the configuration with short-length cylindrical flaps.

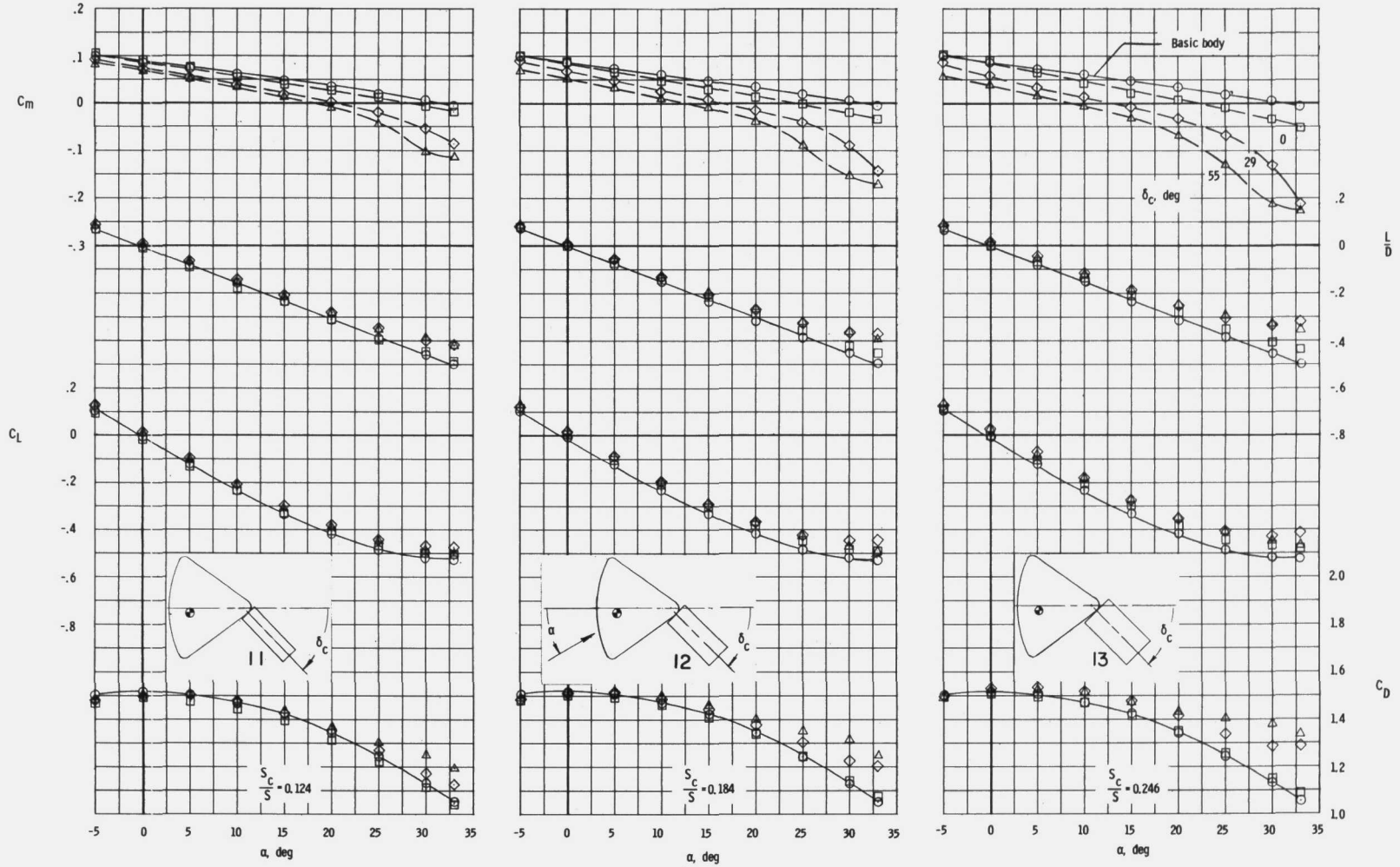



Figure 7.- Longitudinal aerodynamic characteristics of the configuration with medium-length cylindrical flaps.

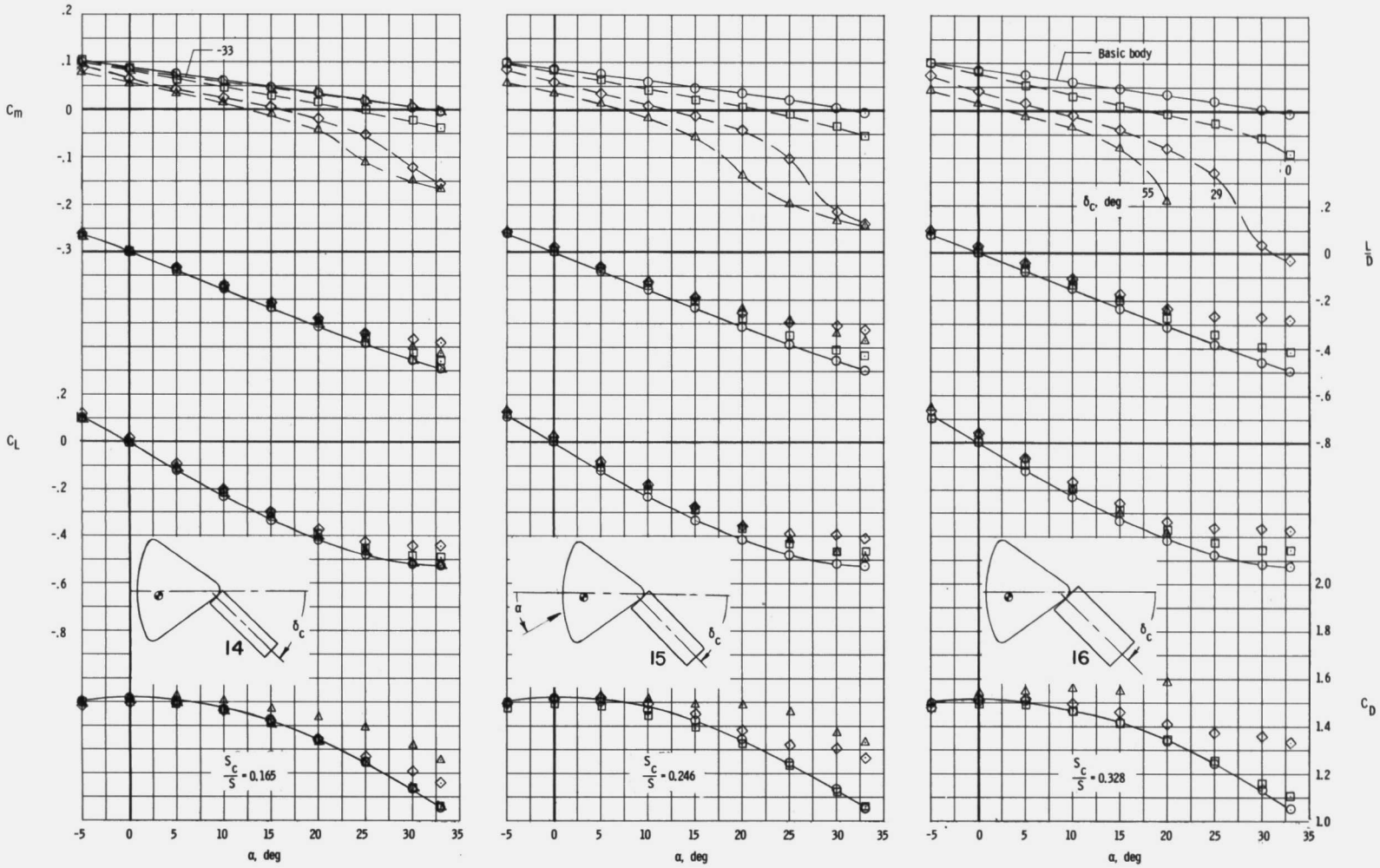
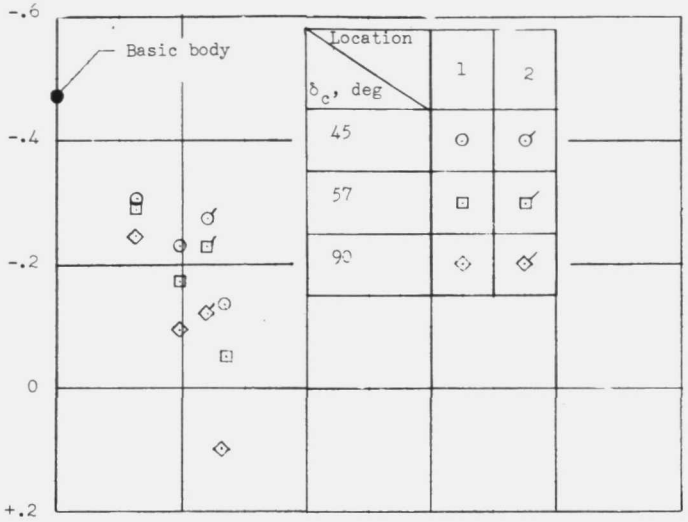
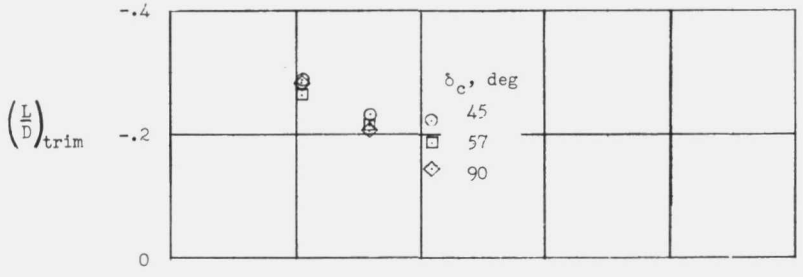


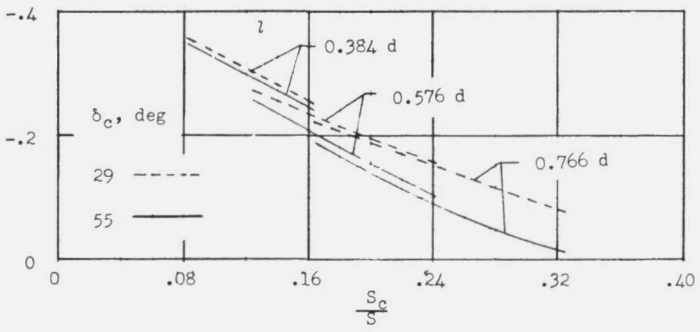

Figure 8.- Longitudinal aerodynamic characteristics of the configuration with long-length cylindrical flaps.




(a) Chin flaps.

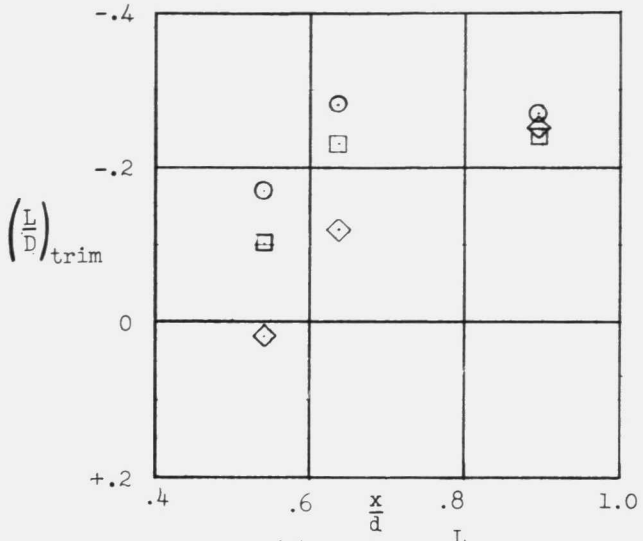


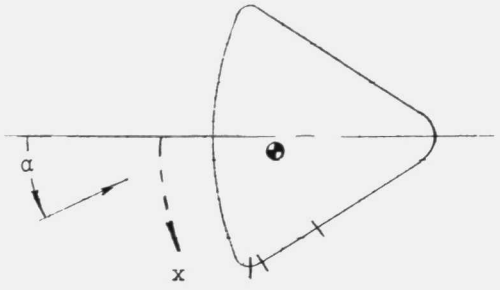

(b) Afterbody flaps.




(c) Cylindrical flaps.

Figure 9.- Effects of control area on trimmed L/D values.



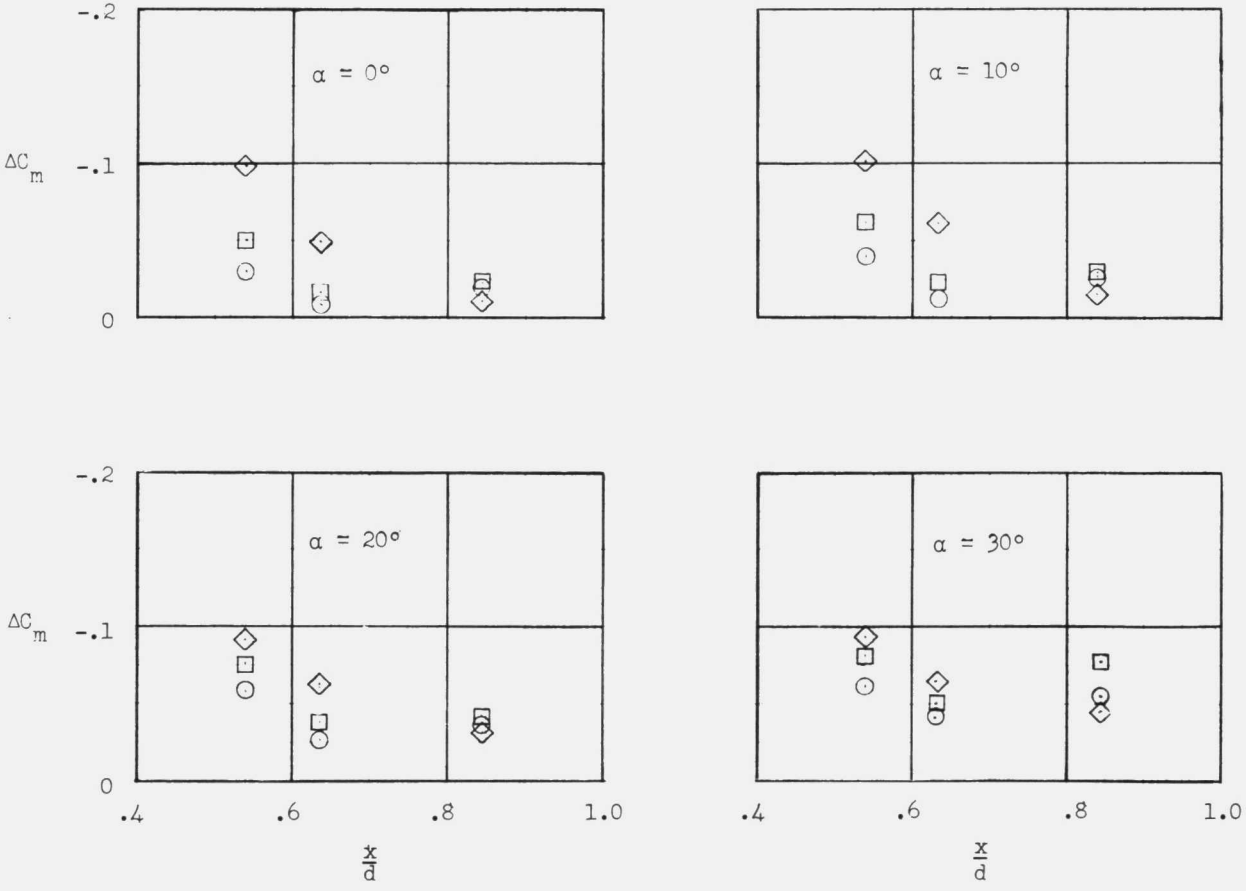

$\delta_c$, deg

○ 45

□ 57

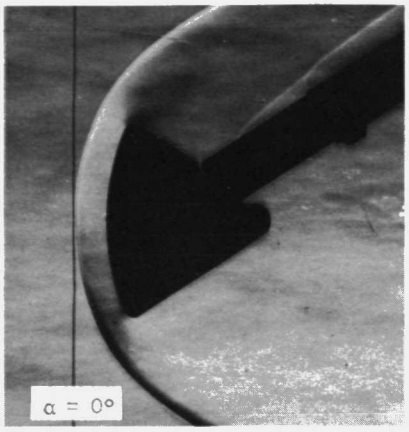
◇ 90

(a) Trimmed $\frac{L}{D}$.

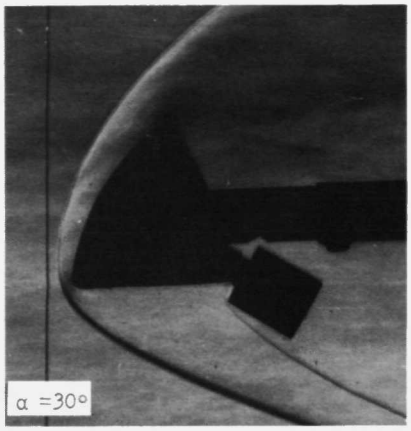



(b) Untrimmed $\Delta C_m$.

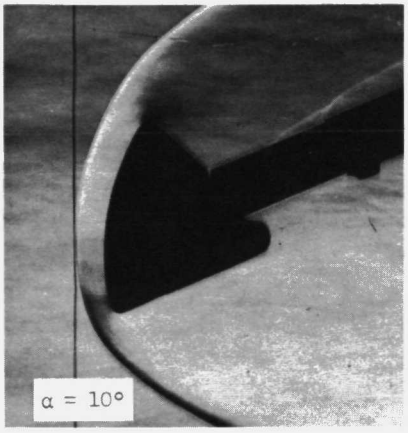
Figure 10.- Effects of location on trimmed L/D and untrimmed $\Delta C_m$. $\frac{S_c}{S} = 0.097$.



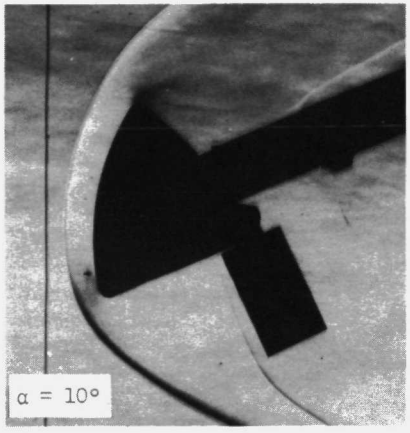

Basic Body



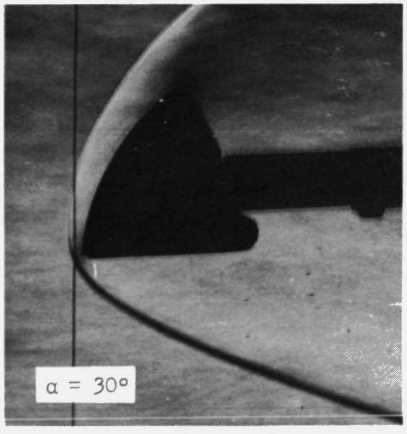

Flap 10; $\delta_c$ = 0°



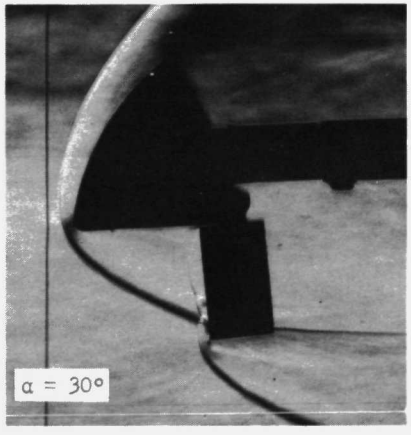

Basic Body




Flap 13; $\delta_c$ = 55°

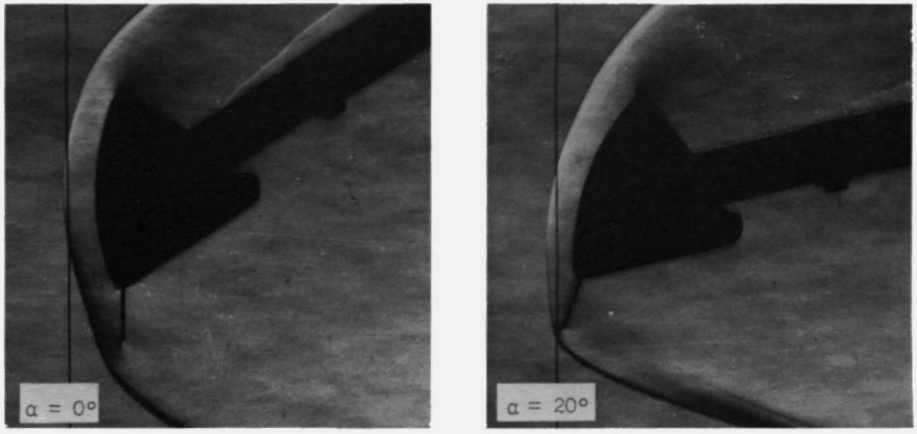



Basic Body

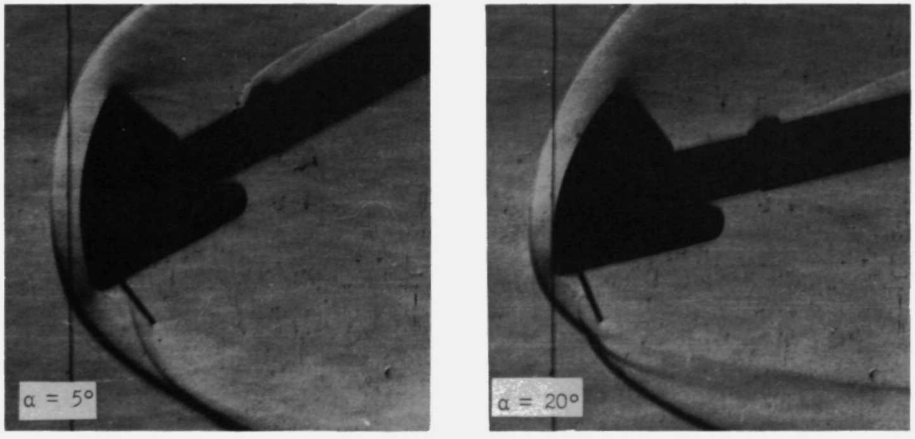



Flap 13; $\delta_c$ = 55°

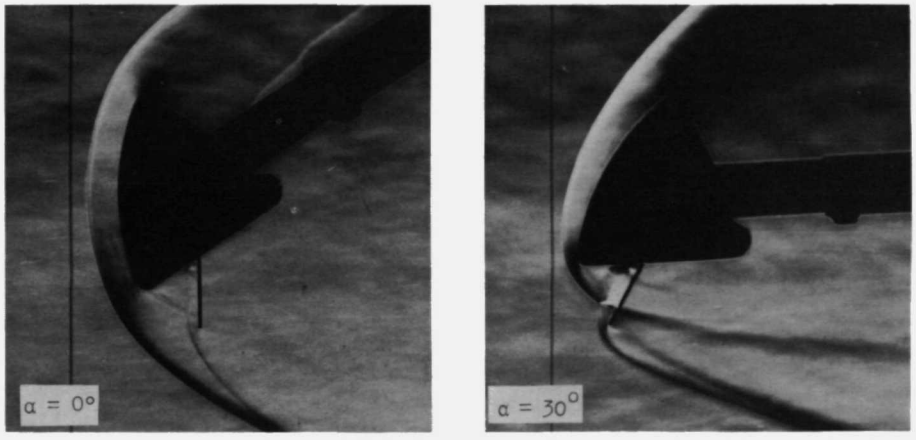
Figure 11.- Schlieren photographs for several configurations. L-63-78




Flap 2; $\delta_c = 90°$




Flap 4; $\delta_c = 47.5°$




Flap 6; $\delta_c = 90°$

Figure 11.- Concluded.

L-63-79